npj | clean water

Comment

Published in partnership with King Fahd University of Petroleum & Minerals

https://doi.org/10.1038/s41545-026-00596-1

# Diverging riverine dissolved C:N:P ratios under global environmental change

Ricky Mwangada Mwanake, Elizabeth Gachibu Wangari, Daniel Graeber & Ralf Kiese



The ratios of dissolved carbon, nitrogen, and phosphorus in rivers constrain downstream carbon and nutrient cycling, yet their long-term trends remain unclear. Using a 20-year ML-modeled dataset spanning 5084 catchments, we show that 27% exhibited coupled C-N-P trends with increasing or decreasing patterns, while 73% exhibited divergent trends. These divergent trends resulted in global declines in DOC-to-nutrient ratios, possibly linked to river warming, anthropogenic land-use expansion, and forest cover declines.

Dissolved organic carbon, total dissolved nitrogen, and total dissolved phosphorus (hereafter DOC, TDN, and TDP) are fundamental building blocks of aquatic life known to regulate key biogeochemical processes in riverine ecosystems[1,2]. This is because their ratios influence whether nutrients are immobilized in biomass or released and transported downstream, with important consequences for river ecosystem functioning[1,3]. For instance, shifts in riverine DOC:nutrient ratios can contribute to adverse downstream environmental effects, including eutrophication, deoxygenation, and increased greenhouse gas emissions from rivers[4–7]. Despite this importance, long-term global trends in riverine DOC:nutrient ratios remain poorly constrained due to a lack of empirical datasets that examine them simultaneously.

Land use and climate change may alter long-term trends in dissolved C:N:P ratios, as both drivers affect DOC, TDN, and TDP mobilization through different pathways and often at different rates[8–10]. For example, agricultural fertilization in intensive agricultural areas and wastewater inputs in urban areas can disproportionately increase TDP or TDN delivery to rivers[8,11–13], while deforestation, soil disturbance, and changes in hydrological connectivity can alter DOC production and export[8,14]. At the same time, climate change may modify dissolved C:N:P ratios by altering temperature, precipitation regimes, and soil organic matter decomposition, thereby affecting both the sources and transport pathways of DOC, TDN, and TDP[15–17]. Apart from their individual effects, land use and climate change drivers may interact, resulting in stronger shifts in riverine DOC:-nutrient ratios. For instance, more intense rainfall may enhance nutrient losses from fertilized or urbanized catchments, while warming and hydrological change may increase DOC mobilization from organic-rich soils, particularly where land management has altered drainage or vegetation structure.

While individual studies have documented rising DOC concentrations in northern headwaters[18], shifting dissolved C:N ratios in streams across biomes[19,20], and strong human impacts on catchment scale C:N:P ratios[10], no study has simultaneously examined long-term temporal trends in DOC:-nutrient ratios at the global scale. As riverine DOC: nutrient ratio imbalances accelerate globally, driven by asymmetrical changes in nutrient inputs[21,22], long-term trends in DOC:nutrient ratios and analyses of their drivers are crucial for predicting how changes in these ratios may affect important downstream carbon and nutrient cycling and loss processes. Here, we aimed to bridge this gap by first investigating the spatial trends in long-term changes in riverine DOC, TDN, and TDP concentrations and their molar ratios. We then examined whether these changes were linked to the expansion of anthropogenic land uses in forests and to warming-induced climatic changes, given that global rivers have warmed by approximately 0.27 °C per decade[23], while anthropogenic land uses and deforestation have, on average, also expanded globally[24]. This analysis leveraged a 20-year (2002–2022) reconstruction of DOC, TDN, and TDP concentrations, generated using random forest models powered by remotely sensed data across 5084 globally distributed catchments[23].

## Results and discussion

Pronounced spatial heterogeneity in the long-term temporal trends of DOC, TDN, and TDP was observed at the global scale, with median annual rates, which also factored in model uncertainties of the three parameters, generally indicating global decreases in riverine DOC and increases in dissolved nutrients (TDN and TDP) (Fig. 1a, c, e). In terms of elemental co-variation, 27% of the catchments exhibited synchronous increases or decreases in DOC, TDN, and TDP concentrations, suggesting that their ratios may have remained relatively stable due to these unidirectional elemental shifts (Fig. S1a). However, the remaining 73% of catchments exhibited divergent trajectories in DOC and nutrient concentrations, indicating decoupled temporal dynamics that alter ratios (Fig. S1b, c).

Among these sites, the patterns were element-specific: 13.6% showed increasing trends in TDP alone (Fig. S1b), with hotspots concentrated primarily in the Amazon Basin of South America (Figs. 1f; S2). This finding agrees with field observations from the Brazilian Amazon, where deforestation and subsequent agricultural expansion have been linked to increased riverine phosphorus concentrations[8]. Increases in TDN alone accounted for 12.5% of sites (Fig. S1b), with hotspot regions concentrated in agriculturally rich areas of Indonesia and Australia, where mineral N fertilization is practiced (Figs. 1c, d; S2). In contrast, the African continent, largely characterized by extensive agricultural systems, exhibited comparatively little to no hotspots for both TDP and TDN increases (Fig. 1d, f). Overall, the largest share of dissolved C, N, and P combinations was associated with declines in DOC (43.1%) rather than increases (30.3%) (Fig. S1). Coldspots representing declining DOC trends were primarily concentrated in agriculturally intensive regions in the South American Amazon basin

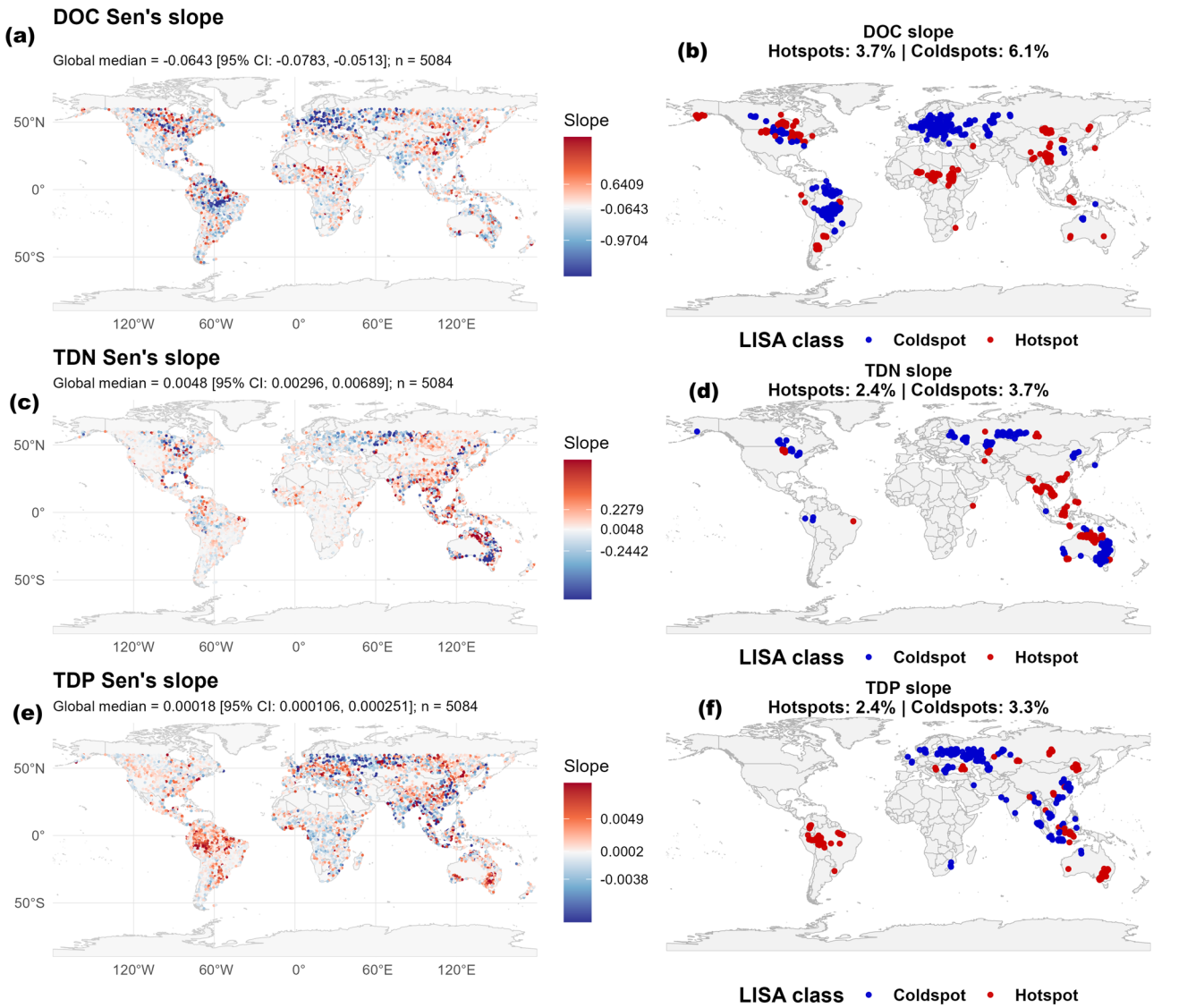


**Fig. 1 | Spatial patterns in temporal trends of dissolved carbon and nutrients in rivers.** Global distribution of the median (±95% CI) annual rates of change for (**a**) DOC, (**c**) TDN, and (**e**) TDP from 2002 to 2022 across 5084 catchments. The median rates were estimated from 1000 Monte Carlo simulations that incorporated model uncertainties. Blue colors indicate declining Sen's slopes, whereas red colors indicate increasing Sen's slopes. **b**, **d**, and **f** show hotspot catchments with steep increasing trends in red and coldspot catchments with steep decreasing trends in blue, identified using the Local Indicators of Spatial Association (LISA) method[35]. The number of hotspots and coldspots is expressed as a percentage of the total number of catchments ($n$ = 5084).

(notably Brazil and Bolivia), Central and Eastern Europe, and parts of China (Fig. 1b).

As a result of the divergent temporal trends in DOC, TDN, and TDP, DOC: nutrient ratios showed either decreasing or increasing trends (Fig. S3), broadly consistent with empirical observations[8,19,25]. However, global median DOC: TDN and DOC: TDP trends indicated that both ratios declined over the past two decades, even after accounting for model uncertainties (Fig. S3). These trends in the ratios are likely driven by simultaneous increases in nutrients and declines in DOC observed at most sites (Figs. 1a, c, e; S3a, b).

We hypothesize that the overall decline in global DOC: nutrient stoichiometric ratios may be governed by distinct but converging mechanisms, i.e., anthropogenic nutrient enrichment in agricultural and urban-dominated catchments[8,10,21,26], declines in DOC concentrations due to deforestation[14] and climate-driven mobilization of organic matter and nutrients in boreal and high-latitude regions[9,17,27]. Consistent with this hypothesis, catchments exhibiting the strongest declines in DOC:TDP ratios were predominantly located in intensively managed agricultural regions in South America, Central Europe, the USA, Canada, and southeastern Australia (Fig. S3d). Catchments with the most pronounced declines in DOC:TDN ratios were distributed across North America, South America, eastern China, and Russia (Fig. S3c). Some of these regions are characterized either by intensive agricultural activity[8] or by boreal and high-latitude systems, where enhanced nutrient mobilization has been shown to be driven by permafrost thaw and hydrological intensification[9,17].

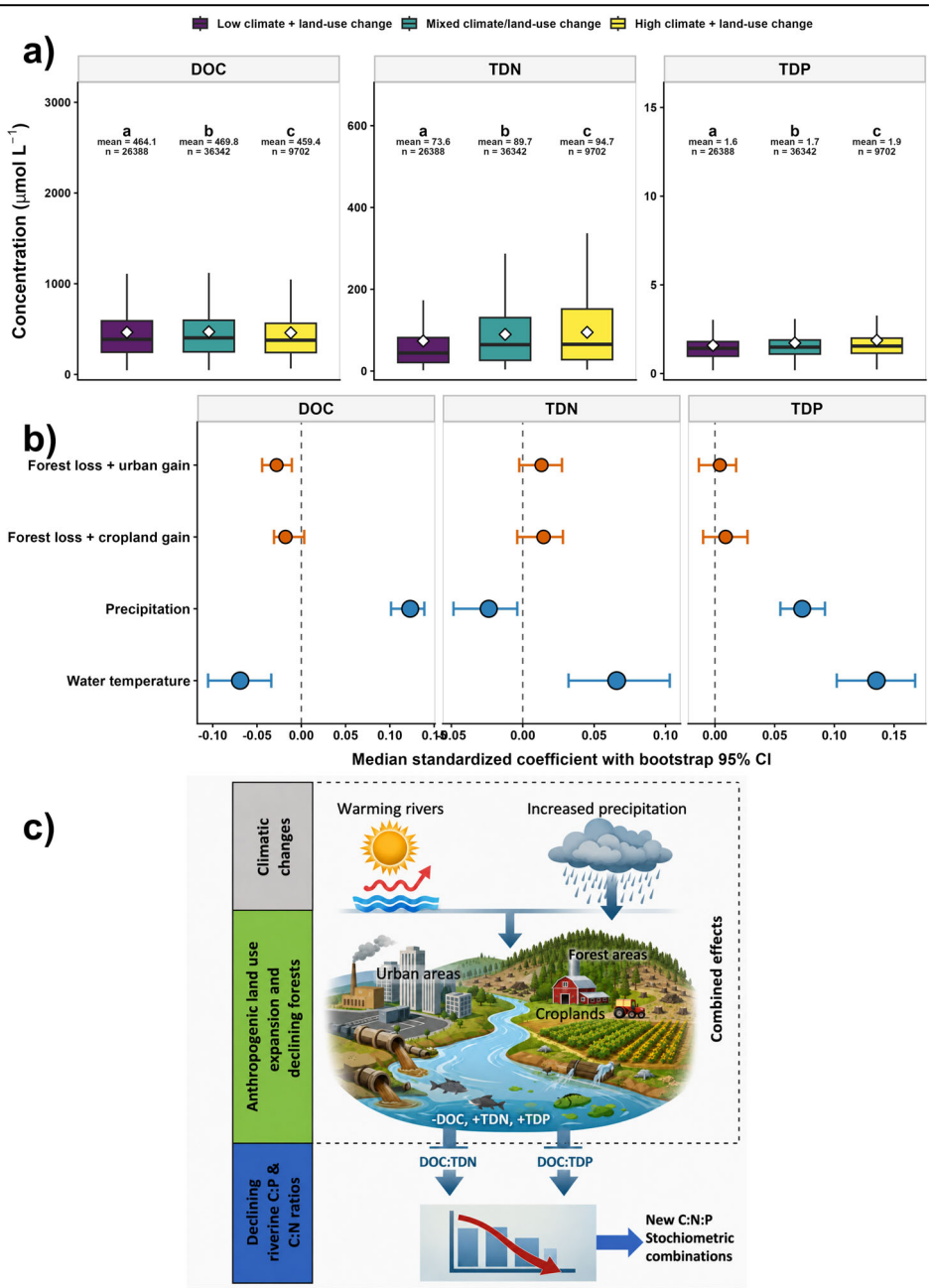


**Fig. 2 | Linking land use and climate variability with trends in riverine dissolved carbon and nutrients. a** Combined effects of climate and land-use change on the variation in riverine DOC, TDN, and TDP concentrations across all sites over the entire study period. Sites were grouped according to compound climate–land-use change classes of low, mixed, and high, with letters above the boxplots indicating significant differences among groups based on pairwise Dunn tests. **b** Site-scale elastic net analysis showing median standardized effect sizes with 95% confidence intervals for the effects of environmental change on temporal variation in DOC, TDN, and TDP concentrations. Predictors were analyzed as standardized continuous variables to evaluate the relative importance of individual climate and land use drivers. **c** Conceptual diagram summarizing the key hypothesis from this study that climatic change, anthropogenic land-use expansion, and declining forest cover may be cumulatively associated with declines in DOC:nutrient ratios in global rivers.

Across all 5084 catchments, DOC:nutrient ratios increased systematically from bulk to organic to inorganic nutrient pools (Fig. S4). This was reflected by the inorganic fraction constituting the minor component of the total nutrient pool (Fig. S5). Median stoichiometric DOC:nutrient ratios were predominantly higher than both the marine phytoplankton (C:N:P = 106:16:1[28]), which represents the autotrophic optimum, and the median ratios characteristic of freshwater microbes (C:N:P = 68:14:1[29]), which represents the heterotrophic optimum (Fig. S4). Such findings suggest strong N and P limitation across global rivers when one assumes complete bioavailability of DOC for both autotrophic and heterotrophic processes. However, this is unlikely to be the case, as evidence from global rivers indicates that, on average, only about 10% of DOC is bioavailable[30]. Such low DOC bioavailability has been shown to strongly constrain heterotrophic reactive N and P uptake rates, as hypothesized by the macronutrient access hypothesis[1]. Assuming a similar DOC bioavailability of ~10%, our results indicate a pronounced limitation of bioavailable DOC on TDN and TDP uptake in global rivers, as the resulting microbially available DOC: nutrient ratios fall below the dual-reference thresholds (Fig. S4). Such findings also agree with empirical evidence from bioavailable DOC addition experiments that increased gross nitrate uptake several-fold in stream biofilms[31], from biofilm and sediment studies linking bioavailable DOC to phosphorus entrapment and self-purification capacity[32], and from

mesocosm experiments that showed increased nitrate uptake and N losses under the addition of bioavalable DOC [3]. Based on these 10%-bioavailability adjusted ratios, we further observe a greater excess of N over P for microbial growth in the global riverine dissolved pool. This asymmetry is consistent with the well-documented global N–P imbalance, driven by the disproportionately rapid increase in anthropogenic reactive N inputs compared to P[22], which has raised environmental N:P ratios across aquatic and terrestrial ecosystems[26].

Despite the apparent disproportionate long-term increase in N relative to P in global rivers, temporal shifts in DOC: nutrient ratios between 2002 and 2022 point to a broader, unifying trend: rivers are gradually becoming more enriched in both nutrients (Fig. S4). To identify the dominant controls underlying the declining temporal trends in DOC:nutrient ratios, we related changes in DOC, TDN, and TDP to concurrent climatic shifts (river warming and precipitation increases), and the declining forest cover due to expansion of upstream anthropogenic land uses, which are key drivers of global environmental change over the past two decades. Catchments experiencing concurrently higher rates of river warming, expanding anthropogenic land use, declining forests and increased precipitation had significantly higher TDN and TDP concentrations and lower DOC concentrations than the catchments experiencing opposite trends in these environmental drivers (Fig. 2a). Moreover, based on the median effect sizes across multiple sites, river warming was positively associated with increases in TDN and TDP concentrations and negatively associated with DOC concentrations. Increases in precipitation was positively associated with DOC and TDP increases and negatively associated with TDN, while forest conversion to anthropogenic land uses mainly coincided with declines in DOC and increases in TDN and TDP (Fig. 2b). Cumulatively, these patterns are consistent with empirical studies showing enhanced mineralization of instream dissolved organic matter or nutrient release from sediments under warmer conditions, or increased nutrient inputs driven by land use, such as fertilizer application, wastewater discharge, and soil erosion, particularly during periods of strong hydrological connectivity between terrestrial and stream ecosystems[15,16,20,26,30,33]. The stronger positive responses of TDN and TDP to climatic and land-use change, compared with DOC as shown above, also suggest that nutrient enrichment may have outpaced carbon enrichment over the past two decades, contributing to the observed decline in riverine DOC:nutrient ratios.

The observed declines in DOC: nutrient ratios, which may be associated with climatic and anthropogenic land use changes, may have direct and cascading consequences for downstream aquatic ecosystems. This is because dissolved C:N:P stoichiometry regulates the balance between microbial catabolic and anabolic processes, thereby influencing whether reactive C, N, and P species are retained (e.g., immobilized in stream sediments and biomass) or exported downstream[3], thus leading to adverse environmental impacts such as eutrophication, deoxygenation, and greenhouse gas emissions. An analysis of our modeled dataset, including GHGs and dissolved oxygen[23], revealed patterns consistent with this mechanistic understanding: an increase in reactive bioavailable DOC increases the supersaturation of riverine $CO_2$, $CH_4$, and $N_2O$, while reducing DO under nutrient excess (Fig. S6). However, when bioavailable DOC is non-limiting (i.e., ratios exceed Redfield proportions), further increases in reactive N and P elicit similar responses, and are associated with increases in both riverine $CO_2$ and $N_2O$ supersaturations and deoxygenation (Fig. S6). Consistent with our modeled results, these mechanisms have also been reported in empirical studies. For example, rivers have been shown to transition from N transformation to N transport and loss-dominated pathways as dissolved C:N ratios narrow, stimulating downstream $N_2O$ production[6,20]. Simultaneously, nutrient enrichment has also been shown to amplify heterotrophic respiration, halving terrestrial C residence times and shifting streams toward net heterotrophy and greater $CO_2$ efflux[4,5]. Nutrient enrichment also results in algal overgrowth, further depleting dissolved oxygen upon decomposition[7]. Collectively, these results demonstrate that both enhanced DOC bioavailability and reactive nutrient enrichment exacerbate riverine degradation.

More broadly, the divergent trajectories of C, N, and P observed may indicate that rivers are transitioning toward novel stoichiometric states not represented in historical records (Fig. 2c). As global change continues to modify both inputs and in situ processing of carbon and nutrients, sustained, coordinated monitoring of dissolved reactive C, N, and P will be essential to identify emerging stoichiometric tipping points, thresholds that our bioavailability-adjusted DOC:nutrient ratios suggest have already been exceeded in many nutrient-enriched streams. This highlights the need for integrated C:N:P management, including the protection of nutrient-poor natural forest and wetland ecosystems that inherently limit bioavailable DOC and constrain downstream adverse environmental impacts. That said, our study is not without limitations; therefore, its findings should be interpreted as hypothesis-generating rather than definitive. For example, the existence of significant uncertainties in the modeled dataset[23], particularly for P forms, which, despite being accounted for in the overall trend analysis, may have affected the magnitudes of the overall trends. Additionally, the analysis of drivers in this study was largely based on correlation analysis with broad catchment-scale patterns associated with climate and land-use gradients, rather than as direct attribution to specific nutrient or carbon sources. Although increasing nutrient concentrations in some regions are consistent with areas known to have fertilized agriculture, potential wastewater inputs, or atmospheric deposition, these mechanisms could not be explicitly separated in this study because high-resolution, temporally consistent global datasets of these parameters were unavailable. Future work combining river chemistry observations with source-specific global datasets will be needed to distinguish the relative contributions of these mechanisms to divergent DOC, TDN, and TDP trajectories.

## Online Methods

**Global dissolved organic carbon and nutrient dataset modeled across 5084 catchments from 2002 to 2022.** In this study, we used a recently published dataset of modeled annual means of riverine dissolved carbon and nutrients (N and P)[23]. This dataset spanned 5084 catchments (excluding desert ecoregions) and included annual mean molar concentrations of DOC, $NO_3$, $NH_4$, TDN, SRP, and TDP. Dissolved organic nitrogen (DON) was calculated as the difference between TDN and dissolved inorganic nitrogen ($DIN = NO_3 + NH_4$), while dissolved organic phosphorus (DOP) was calculated as the difference between TDP and SRP.

In brief, the modeled dataset was generated using random forest models trained on an empirical global dataset comprising measurements from up to 1085 sites across six continental regions (South America, North America, Africa, Australia, Europe, Asia), sampled between November 2000 and April 2022[23]. Predictors in the models were exclusively catchment-scale remote-sensing datasets, including daily vegetation indices, namely NDVI, NDWI, and EVI, the snow cover index (NDSI), the burn area index (BAI), three-hourly average photosynthetically active radiation (PAR), elevation, stream order, and a topographic diversity variable. These predictors were selected because they were available at global and/or daily resolutions that matched the empirical dataset used to calibrate and validate the random forest models[23]. They also provided process-relevant proxies for catchment-scale controls on dissolved carbon and nutrient dynamics in rivers. For example, vegetation indices may represent terrestrial productivity, and potential organic matter and nutrient inputs to rivers, while PAR reflects

light availability and its influence on instream photosynthesis and respiration. Stream order represents terrestrial–aquatic connectivity, whereas elevation and topographic diversity represent broader landscape heterogeneity.

Based on an analysis of the best-performing predictors, these variables also showed relationships with DOC and nutrient species that matched the expected mechanistic relationships reported in other studies (Fig. S7). For example, the topographic diversity variable, a potential proxy for biodiversity, was negatively associated with fluvial TDN and $NH_4$. This suggests that more heterogeneous and potentially more biodiverse landscapes may have lower fluvial nutrient concentrations than less diverse, more human-influenced catchments[12]. Similarly, the negative relationship between stream order and TDN agrees with established hydrological and biogeochemical mechanisms. Smaller streams often show stronger connectivity with groundwater and surrounding terrestrial ecosystems and may therefore receive proportionally higher nitrogen inputs than larger rivers[34]. In contrast, SRP and TDP increased with stream order, suggesting that downstream sediment accumulation and associated phosphorus release may contribute to higher phosphorus concentrations in larger river reaches[13]. Relationships involving vegetation indices also supported mechanistic interpretations. For instance, the positive association between NDVI and DOC suggests that higher terrestrial productivity, which increases organic matter inputs, may enhance DOC concentrations in surface waters.

Model performance ranged from moderate to high ($R^2$: 0.44-0.90). Independent validation using 30% of the global empirical dataset showed that the models generally reproduced observed daily concentration patterns well, with observed-versus-predicted $R^2$ values reaching up to 0.90 (Fig. S8). The lowest observed-versus-predicted $R^2$ values were found for SRP and TDP, likely due to model deviations that were most pronounced at extremely low and high concentrations, although most data points remained clustered around the 1:1 line. Model uncertainties for each parameter were expressed as the percentage of the mean absolute error relative to the parameter's observed global mean. These uncertainties ranged from 6.8% to 75.7%, with DOC predictions having the lowest and SRP the highest (Table S1). These differences in uncertainty were driven by both the number of measurements used for training, which was lower for SRP than for DOC, and the magnitude of the concentrations, particularly the very low SRP values. Temporal skill at the site scale was assessed using the Kling–Gupta Efficiency (KGE) metric across all sites. The advantage of the KGE metric is that it integrates correlation, bias, and variability into a single score, providing a more balanced evaluation by explicitly including these different measures of error. KGE values ranged from 0.18 to 0.61, with an overall average of 0.42 (Table S1). After these steps, we then used the daily-trained and validated random forest models for each parameter to reconstruct the annual global trends in DOC, TDN, TDP, $NH_4$, and $NO_3$ for the period 2002-2022 based on remote-sensing observations[23]. Detailed information about the modeled data generation can be found in the respective publication[23].

**Temporal trends in DOC, TDN, and TDP and their ratios.** To assess temporal changes in riverine dissolved carbon, nitrogen, and phosphorus, we quantified site-level trends for DOC, TDN, and TDP concentrations and their ratios. These temporal trends were estimated over the 20-year study period using Sen's slope estimator, which is less sensitive to outliers than standard linear regression, providing annual rates of change for DOC, TDN, and TDP concentrations, as well as DOC:TDN and DOC:TDP ratios. To account for the uncertainty in the modeled concentration estimates, we first propagated variable-specific relative uncertainties through the trend analysis using a Monte Carlo framework. In this analysis, uncertainty values of 6.8% for DOC, 13.5% for TDN, and 47.2% for TDP were used (Table S1). Specifically, site-scale annual DOC, TDN, and TDP values were varied 1000 times within their respective uncertainty estimates, and their ratios were calculated for each simulation. Sen's slopes were then estimated for each element and ratio within each simulation. The median of the resulting slope distribution ($n = 1000$) was used as the site-level trend estimate, with the 5th and 95th percentiles representing uncertainty bounds. These Monte Carlo-derived median slopes were used as the main slope estimates for mapping and spatial analyses.

**Identification of temporal hotspots and coldspots.** Hotspots and coldspots in the temporal trends of DOC, TDN, and TDP, as well as their derived ratios, were identified using Local Indicators of Spatial Association (LISA) based on Local Moran's I[35]. First, Monte Carlo-derived median slopes were spatially represented as point features and projected to a metric coordinate reference system to ensure accurate distance calculations. Spatial relationships among sites were defined using a k-nearest neighbors approach (k = 8), and row-standardized spatial weights were constructed. Local Moran's I statistics were computed for each variable to assess the degree of local spatial autocorrelation between each catchment and its neighbors. Sites were classified into LISA cluster types based on the sign of the centered variable and its spatial lag, combined with statistical significance ($\alpha = 0.05$). Specifically, hotspots (high–high clusters) represent sites with above-average trends surrounded by similarly high values, whereas coldspots (low–low clusters) indicate sites with below-average trends surrounded by low values. Non-significant locations and spatial outliers were excluded. The proportion of hotspots and coldspots was calculated relative to the total number of sites for each variable and ratio, providing a quantitative measure of spatial clustering in temporal dynamics. To characterize multi-element trajectory classes, we independently assessed the Monte Carlo-derived median slopes trends for DOC, TDN, and TDP concentrations at each site and combined them into composite C–N–P trends (e.g., all increasing, all decreasing, C up/N down/P up). The proportion of sites in each class was calculated and mapped globally.

To evaluate how the combined dissolved C:N:P stoichiometry changed over the study period, we compared modeled concentrations at the start (2002) and end (2022) of the 20-year period. This was done by computing six molar stoichiometric ratios representing bulk (DOC:TDN, DOC:TDP), organic (DOC:DON, DOC:DOP), and inorganic (DOC:DIN, DOC:SRP) nutrient pools for each site in both years. The distributions of these ratios were visualized as paired violin plots, and the medians compared with two reference benchmarks, i.e., the marine Redfield ratio for phytoplankton (C:N:P = 106:16:1)[28] representing the autotrophic optimum and the freshwater DOM benchmark of Godwin & Cotner (2018) for lake-derived heterotrophic planktonic bacteria strains (C:N:P = 68:14:1)[29] representing the heterotrophic optimum. This dual-anchor comparison enabled an ecological assessment of whether riverine dissolved combined C:N:P stoichiometry deviates from known reference values and whether these deviations have shifted over two decades, as has been done in past studies[10].

**Analysis of the effects of environmental changes on DOC, TDN, and TDP.** To evaluate how dissolved C, N, and P concentrations varied across combined environmental-change contexts, sites were classified according to combined climate and land use changes. Site-level temporal trends were calculated for water temperature, precipitation, and land use variables (urban, cropland, and forested areas). The precipitation data were sourced from the CHIRPS dataset (https://developers.google.com/earth-engine/datasets/catalog/UCSB-CHG_CHIRPS_DAILY#bands), land use

data from the HILDA+ dataset[24], and the water temperature data from a global water temperature reconstruction[23]. Sen's slopes for each driver were standardized (z-score standardization) across sites to allow comparison among variables with different units. A climate-change z-score was calculated as the sum of the temperature and precipitation standardized slopes. A land-use-change z-score was calculated as the difference between the sum of the standardized urban and cropland slopes and the standardized forest slope. The rationale for these combinations is that climate change is expected to result in warmer rivers and more frequent extreme precipitation events[23], whereas anthropogenic land-use change is characterized by urban and agricultural expansion alongside declining forest cover[24]. Thus, positive land-use-change scores indicate catchments with increasing urban and/or cropland cover and decreasing forest cover. Based on these two scores, sites were then classified as having high or low climate change and high or low land-use change using the median value of each score as the threshold. These classes were combined into three compound-change groups: low climate + land-use change, mixed climate/land-use change (low-high mixture of either change), and high climate + land-use change. Significant differences in DOC, TDN, and TDP among these combined environmental change classes were then determined using pairwise non-parametric Dunn tests.

Apart from analyzing these general trends, we also evaluated the relative importance of climatic and land-use predictors at catchment scales. Specifically, site-level elastic net models were fitted separately for DOC, TDN, and TDP. Predictors in these models included water temperature, precipitation, and land-use transitions from forest to cropland and from forest to urban. The two land use transitions were calculated annually relative to the first observation at each site. Forest loss was calculated as the positive decline in forest cover from the initial observation, whereas cropland gain and urban gain were calculated as positive increases in cropland and urban cover from the initial observation. For each site-level model, the response and predictors were standardized within the site prior to model fitting. Elastic net models were used because they can evaluate several correlated environmental predictors simultaneously while reducing the influence of weak or redundant predictors. The elastic net mixing parameter was set to $\alpha = 0.5$, giving a balance between ridge-type shrinkage, which stabilizes estimates when predictors are correlated, and lasso-type selection, which allows less informative predictors to be reduced to zero. Cross-validation was used to identify the amount of regularization that minimized prediction error. The coefficient estimates from this minimum-error solution were used as the main model output because they retained more information on site-level predictor effects. For each predictor and response variable, coefficient summaries were calculated across cross-validated site-level models. The main reported effect size was the median standardized coefficient, with bootstrap 95% confidence intervals.

## Data availability

The data that support the findings of this study are openly available in Zenodo at https://doi.org/10.5281/zenodo.19202635.

**Ricky Mwangada Mwanake[1] ✉, Elizabeth Gachibu Wangari[1], Daniel Graeber[2] & Ralf Kiese[1]**

[1]Karlsruhe Institute of Technology, Institute for Meteorology and Climate Research, Atmospheric Environmental Research (IMK-IFU), Garmisch-Partenkirchen, Germany. [2]Department of Aquatic Ecosystem Analysis and Management, Helmholtz-Centre for Environmental Research– UFZ, Magdeburg, Germany. ✉e-mail: ricky.mwanake2@kit.edu

Received: 29 April 2026; Accepted: 3 June 2026;
Published online: 08 June 2026

## References

1. Graeber, D. et al. Bioavailable DOC: reactive nutrient ratios control heterotrophic nutrient assimilation—An experimental proof of the macronutrient-access hypothesis. *Biogeochemistry.* **155**, 1–20 (2021).
2. Mwanake, R. M. et al. Natural abundance sediment δ15N as a proxy for long-term gross N-turnover processes, GHG emissions, and denitrification hotspots within fluvial ecosystems. *Environ. Adv.* **23**, 100685 (2026).
3. Große, A. et al. Stream C to N to P ratios aligned with microbial needs enhance biofilm nitrate uptake and subsequent nitrogen loss. *Biogeochemistry.* **168**, 62 (2025).
4. Cross, W. F. et al. Nutrient enrichment intensifies the effects of warming on metabolic balance of stream ecosystems. *Limnol. Oceanogr. Lett.* **7**, 332–341 (2022).
5. Rosemond, A. D. et al. Experimental nutrient additions accelerate terrestrial carbon loss from stream ecosystems. *Science (1979)* **347**, 1142–1145 (2015).
6. Mwanake, R. M. et al. Elevated in-stream $CO_2$ concentration stimulates net-N2O production from global fluvial ecosystems. *Water Res.* **287**, 124320 (2025).
7. Wurtsbaugh, W. A., Paerl, H. W. & Dodds, W. K. Nutrients, eutrophication and harmful algal blooms along the freshwater to marine continuum. *WIREs Water* **6**, e1373 (2019).
8. Biggs, T. W., Dunne, T. & Martinelli, L. A. Natural controls and human impacts on stream nutrient concentrations in a deforested region of the Brazilian Amazon basin. *Biogeochemistry* **68**, 227–257 (2004).
9. Kraus, K. L. & Jones, J. B. Long-term stream chemistry patterns in a boreal watershed underlain with discontinuous permafrost. *J. Geophys. Res. Biogeosci.* **130**, e2025JG009126 (2025).
10. Wachholz, A. Stoichiometry on the edge—humans induce strong imbalances of reactive C:N:P ratios in streams. *Environ. Res. Lett.* **18**, 044016 (2023).
11. Mwanake, R. M., Gettel, G. M., Wangari, E. G., Butterbach-Bahl, K. & Kiese, R. The role of agricultural fertilization intensity on fluvial GHG fluxes from tropical and temperate catchments. https://doi.org/10.1016/j.jenvman.2025.127782 (2025).
12. Upadhyay, P., Prajapati, S. K. & Kumar, A. Impacts of riverine pollution on greenhouse gas emissions: A comprehensive review. *Ecol. Indic.* **154**, 110649 (2023).
13. Bowes, M. J., House, W. A. & Hodgkinson, R. A. Phosphorus dynamics along a river continuum. *Sci. Total Environ.* **313**, 199–212 (2003).
14. Drake, T. W. et al. Mobilization of aged and biolabile soil carbon by tropical deforestation. *Nat. Geosci.* **12**, 541–546 (2019).
15. Zhou, X., Chen, N., Yan, Z. & Duan, S. Warming increases nutrient mobilization and gaseous nitrogen removal from sediments across cascade reservoirs. *Environ. Pollut.* **219**, 490–500 (2016).
16. Duan, S.-W. & Kaushal, S. S. Warming increases carbon and nutrient fluxes from sediments in streams across land use. *Biogeosciences* **10**, 1193–1207 (2013).
17. Francis, A. et al. Permafrost degradation and nitrogen cycling in Arctic rivers: insights from stable nitrogen isotope studies. *Biogeosciences* **20**, 365–382 (2023).
18. Monteith, D. T. et al. Long-term rise in riverine dissolved organic carbon concentration is predicted by electrolyte solubility theory. *Sci. Adv.* **9**, eade3491 (2023).
19. Rodríguez-Cardona, B. M. et al. Shifting stoichiometry: Long-term trends in stream-dissolved organic matter reveal altered C:N ratios due to history of atmospheric acid deposition. *Glob. Chang. Biol.* **28**, 98–114 (2022).
20. Wymore, A. S. et al. Gradients of anthropogenic nutrient enrichment alter N composition and DOM stoichiometry in freshwater ecosystems. *Glob. Biogeochem. Cycles* **35**, e2021GB006953 (2021).
21. Manning, D. W. P., Rosemond, A. D., Benstead, J. P., Bumpers, P. M. & Kominoski, J. S. Transport of N and P in U.S. streams and rivers differs with land use and between dissolved and particulate forms. *Ecol. Appl.* **30**, e02130 (2020).
22. Peñuelas, J. & Sardans, J. The global nitrogen-phosphorus imbalance. *Science (1979)* **375**, 266–267 (2022).
23. Mwanake, R. M., Wangari, E. G. & Kiese, R. Rising global riverine deoxygenation rates and GHG emissions driven by the synergistic effects of warming and anthropogenic land use expansion. *Glob. Chang. Biol.* **32**, e70828 (2026).
24. Winkler, K., Fuchs, R., Rounsevell, M. & Herold, M. Global land use changes are four times greater than previously estimated. *Nat. Commun.* **12**, 2501 (2021).
25. Shousha, S., Maranger, R. & Lapierre, J. Decadal changes in anthropogenic inputs and precipitation influence riverine exports of carbon, nitrogen, and phosphorus, and alter ecosystem level stoichiometry. *Glob. Biogeochem. Cycles* **37**, e2023GB007820 (2023).
26. Peñuelas, J. et al. Human-induced nitrogen–phosphorus imbalances alter natural and managed ecosystems across the globe. *Nat. Commun.* **4**, 2934 (2013).
27. Li, Z. et al. Accelerated soil phosphorus cycling upon abrupt permafrost thaw. *Nat. Clim. Chang.* **15**, 1234–1240 (2025).
28. Redfield, A. The biological control of chemical factors in the environment. *Am. Sci.* **46**, 205–221 (1958).
29. Godwin, C. M. & Cotner, J. B. What intrinsic and extrinsic factors explain the stoichiometric diversity of aquatic heterotrophic bacteria? *ISME J.* **12**, 598–609 (2018).
30. Stutter, M. I., Graeber, D., Evans, C. D., Wade, A. J. & Withers, P. J. A. Balancing macronutrient stoichiometry to alleviate eutrophication. *Sci. Total Environ.* **634**, 439–447 (2018).
31. Stutter, M., Graeber, D. & Weigelhofer, G. Available dissolved organic carbon alters uptake and recycling of phosphorus and nitrogen from river sediments. *Water* **12**, 3321 (2020).
32. Perujo, N. et al. Bioavailable dissolved organic carbon serves as a key regulator of phosphorus dynamics in stream biofilms. *Environ. Microbiol. Rep.* **17**, e70115 (2025).
33. Bian, Z. et al. Extreme precipitation reshapes nutrient flows and balance in North America's largest river basin. *Sci. Adv.* **12**, eaea3260 (2026).

34. Mwanake, R. M. et al. Basin-scale estimates of greenhouse gas emissions from the Mara River, Kenya: Importance of discharge, stream size, and land use/land cover. *Limnol. Oceanogr.* **67**, 1776–1793 (2022).
35. Anselin, L. Local Indicators of Spatial Association—LISA. *Geogr. Anal.* **27**, 93–115 (1995).

## Acknowledgements
The TERENO Bavarian Alps/Pre-Alps Observatory provided infrastructure funding for this study, which was supported by the Helmholtz Association through the joint Changing Earth—Sustaining our Future (PoF IV) program of the Karlsruhe Institute of Technology (KIT).

## Author contributions
Conceptualization: R.M.MMethodology: R.M.M., E.G.WInvestigation: R.M.M., D.G., and R.K.Visualization: R.M.M.Writing – review & editing: All authors.

## Competing interests
The authors declare no competing interests.

## Additional information
**Supplementary information** The online version contains supplementary material available at https://doi.org/10.1038/s41545-026-00596-1.

**Correspondence** and requests for materials should be addressed to Ricky Mwangada Mwanake.